SUPPLEMENTARY METHODS

Immunochemistry in primary culture neurons

Primary neurons from bioUb and UBE3A-OE mice brain at P0-P1 were cultured as previously described (Beaudoin *et al.*, 2012). After 14 days of maintenance, cultured mouse neurons were immunostained and mounted on coverslip following the protocol previously described (Beaudoin et al., 2012). We used mouse monoclonal anti-UBE3A from Sigma at 1:100 as primary antibody combined with the secondary fluorescent-conjugated antibody Alexa Fluor 647 chicken anti-mouse from Invitrogen at 1:1000. The coverslips were mounted using Fluoromont-G with DAPI from Invitrogen and neurons were imaged with a Zeiss LSM 880 confocal microscope (Carl Zeiss AG, Jena, Germany). Analysis of confocal images was done to measure the nuclear/cytoplasmic fluorescence ratio using ImageJ distribution Fiji (Schindelin et al., 2012). DAPI signal was use to delimit nucleus and mean fluorescent intensity (MFI) was calculated for cytoplasm and the nucleus. Background MFI was calculated as the average MFI of three different areas surrounding the neurons and was subtracted. All analysis was done blind for neuron genotype.

Behavioural tests

Ube3a$^{+/+}$ mice and age-matched controls (C57BL/6 background) were used for behavioural experiments. Animals were housed 4-5 per cage on a 12-12 h light/dark cycle, at 21-23°C and 65-70% humidity. Food and water were provided ad libitum. Animal maintenance and experimental procedures were executed in accordance with the guidelines of animal care established by the European Communities Council Directive 2010/63/EU, as well as in agreement with the Spanish Legislation (Royal Decree 53/2013). Procedures were also approved by the UPV/EHU Institutional Ethics Committee for Animal Welfare (CEEA). Behavioural tests relevant to autism were performed as in Silverman et al. (2010) as follows:

Ultrasonic Vocalizations (UsV). P7 pups were removed from the dam and placed in individual heated sound-proof chambers equipped to record UsV for 5 min. UsV were analyzed with Avisoft sound analysis software for laboratory animals.

Reciprocal social interaction test. P21-28 mice were placed in a cage to which they had been previously habituated with an unfamiliar mouse matched in age, genotype, and sex for 10 min. The time engaged in social interaction (nose-to-nose sniffing, nose-to-anus sniffing, and following or crawling on/under each other) for the pair (combining the behaviour of both animals) was measured by two independent experimenters.

Open Field. P30 mice were placed inside a clear Plexiglas arena for 20 min, and their general locomotor activity (distance travelled and velocity) was recorded. Results were analyzed with ANY-maze behaviour tracking software.

Grooming. Grooming behaviour was manually measured at P30 by isolating mice in regular housing cages during 10 min.

Social approach (three-chamber) test. The social approach test was performed at P35-42. After allowing the mouse to inspect the empty 3-chamber arena for 10 min as habituation, it was placed in the central chamber of a clear Plexiglas box divided into three interconnected chambers and was given the choice to interact with either an empty wire cup (located in one side chamber) or a similar wire cup with an unfamiliar mouse inside (located in the opposite chamber), which was matched in age and sex. Time interacting with each cup was measured by two independent experimenters.

Light-dark box. At P45, mice were placed for 10 min in a box with a small dark safe compartment and a large aversive compartment illuminated with bright light. The time to exit the dark area was measured as indicative of their anxiety levels.

In vitro ubiquitination assay

Reaction mixtures contained purified enzymes (20 nM E1 UBE1 (Biotechne), 250 nM E2 UBE2L3 (Biotechne) or UBE2N (enQuirebio) or UBE2N-UBE2V1 complex (Millipore), and 250 nM E3 UBE3A (Biotechne) and 1.25 µM of ubiquitin (R&D Systems) in 50 µl of reaction buffer (25 mM Tris-HCl pH 7.6, 5 mM $MgCl_2$, 100 mM NaCl, 2 mM ATP). Samples were incubated at 37ºC. At the indicated time points reactions were stopped by adding 50 µl of Laemmli buffer with reducing agent DTT and boiled 5 min before loading on SDS-polyacrylamide gel. Detection was performed by immunoblotting using mouse monoclonal anti-UBE3A antibody (Sigma, 1:1000 dilution).

SUPPLEMENTARY FIGURE LEGENDS

Supplementary Figure 1. (A) Simplified comparison of all known mouse and human UBE3A isoforms. The UBE3A-OE mouse presented in this work should overexpress both the long (isoform 2) and short (isoform 3) mouse isoforms. Identical sequences are shown in red; the extended sequences for long UBE3A isoforms are shown in blue or orange. Lines connect corresponding isoforms from each species. (B) Full western blots of anti-UBE3A on total brain from four independent biological replica extracts confirm the UBE3A overexpression in UBE3A-OE mice brains compared to UBE3A endogenous levels in BirA and bioUb samples. (C) Primary neuronal cultures of bioUb (labeled Control) and UBE3A-OE mice immunostained for UBE3A (magenta) and DAPI (blue) and quantification of the ratio of nuclear to cytoplasmic fluorescent expression of UBE3A. Scale bar = 50 μm. Inset shows representative neuron used for analysis. Scale bar = 10 μm.

Supplementary Figure 2. (A) Behavioural tests assessing social behaviour show no alterations in the number of isolation-induced ultrasonic vocalizations in UBE3A-OE mice, nor in the reciprocal social test or the social approach test. (B) Overexpression of UBE3A increases repetitive behaviour as denoted by the time spent grooming in a 10min test (C) Open field test Measurement of the distance travelled (left) and velocity (right) identifies increased locomotor activity in UBE3A-OE mice (D) Dark-light box test. UBE3A-OE mice show a shorter latency to enter a bright open area, which might indicate reduced anxiety. (E) UBE3A-OE mice show normal sensory reactivity to a hot plate. Data are represented as mean ± SEM. *$p < 0.05$, **$p < 0.01$. Statistical significance was calculated by independent samples t-test.

Supplementary Figure 3. (A) Multiscatter plots correlating the TMT values of all 6 samples, before normalization with median subtraction. Similarity between replicas of the same experimental condition ($r \approx 0.99$) was just slightly higher than between the different experimental conditions ($r \approx 0.97$). (B) Anti-BirA immunoblot on total brain extracts indicates that appropriate processing of the bioUb precursor was performed by endogenous deubiquitylases in both bioUb and UBE3A-OE samples. (C) Anti-biotin western blot performed for each of the genotypes in total (Input) and purified (Elution) brain extracts. In the BirA control samples mainly two bands corresponding to endogenously biotinylated proteins PCB (~130kD) and PCCA (~80kD) are detected. In bioUb samples, a single band around 10 KDa and an additional smear due to conjugation of bioUb to many cellular substrates are

observed. Very similar pattern is observed in both total brain lysates and in the bioUb pull-down samples. (D) Immunoblotting with FK1 and FK2 antibodies to polyubiquitin (specific to different ubiquitin-conjugated forms) confirms that the isolated proteins include different types of ubiquitin chains, with no significant differences between the ubiquitinated material isolated from bioUb and UBE3A-OE mice brains. (E) Silver staining reveals a massive enrichment of ubiquitinated material on both bioUb and UBE3A-OE samples, while the BirA samples are mostly enriched for two endogenously biotinylated carboxylases. (F) Full Western blots with anti-UBE3A antibodies on purified brain extracts from four independent biological replicas.

Supplementary Figure 4. (A) Western Blot anti-biotin performed on the isolated material from biotin pull-downs used for MS analysis. Dilutions of the inputs (1/10), flow-throughs (FT; 1/10) and elutions (1/100) are shown for each genotype. Biotinylation and conjugation of the ectopic biotinylated ubiquitin is properly accomplished in both mice expressing bioUb. (B) Silver staining on 10% of the material purified from each biological replica. Equal amount of control and UBE3A-OE samples from each pull-down replica were resolved in a 4-12% gradient polyacrylamide gel and stained with silver. (C) In order to detect by MS the proteins isolated by Neutravidin pull-down, samples were first fractionated by SDS-PAGE, Coomassie-stained and all gel lanes cut into four slices. (D) Venn diagrams showed a very high overlap between proteins identified across replicas of the same experimental conditions. (E) Multiscatter plots correlating the non-imputed LFQ values of all 6 samples indicate that the similarity between distinct replicas of the same experimental condition is higher ($r \approx 0.99$) than between distinct datasets ($r \approx 0.89$). (F) Anti-UBA1 antibody reveals a similar amount of active E1 enzyme being present in both bioUb elution samples. (G) Immunoblots at different time points of the *in vitro* UBE3A autoubiquitination assays indicate that, besides UBE2L3, UBE2N is also an E2 enzyme for UBE3A, but it requires the presence of its cofactor UBE2V1 to effectively ubiquitinate the substrate. Two independent experimental replicas are shown.

Supplementary Figure 5. (A) Venn diagram showing overlap of quantitative protein identification between experimental conditions. Small circles represent significantly enriched (orange) and depleted (orange) proteins. (B) A correlation plot of total protein abundance and ubiquitinated fraction abundance fold enrichment upon UBE3A overexpression for these proteins identified as UBE3A substrates reveal no correlation. UBE3A itself can be seen enriched in both data sets. A negative correlation would be expected if proteasome-targeted

ubiquitination of UBE3A substrates would alter significantly the total abundance of these proteins.

Supplementary Figure 6. Compilation of all Western Blots performed on UBE3A substrates.

SUPPLEMENTARY TABLE LEGENDS

Supplementary Table 1. TMT and LFQ based identified and quantified proteins. (A) Proteins identified by LC-MS/MS in whole brain samples and biotin-based pull-downs, by TMT and LFQ, respectively. (B) Proteins significantly enriched and depleted in whole brain samples upon overexpression of UBE3A, as determined by TMT quantification. (C) Active UPS enzymes identified by LC-MS/MS in biotin-based pull-downs, as determined by LFQ quantification. (D) Other UPS components identified by LC-MS/MS in biotin-based pull-downs, as determined by LFQ quantification. (E) Proteins significantly enriched and depleted in biotin-based pull-downs upon overexpression of UBE3A, as determined by LFQ quantification. (F) UBE3A-mediated ubiquitinated proteins identified by LC-MS/MS in biotin-based pull-downs, as determined by LFQ quantification. (G) Putative UBE3A substrates, after application of exclusion criteria. (H) Excluded UBE3A substrates based on permutation-based FDR and Benjamini-Hochberg tests. (I) Full Table 1 with selected substrates complying with all three statistical thresholds and identified in both control and UBE3A-OE samples. (J) Selected UBE3A substrates complying with all three statistical thresholds but identified only in UBE3A-OE samples.

Supplementary Table 2. Validation of putative UBE3A substrates by PRM-based targeted proteomics. List of peptides monitored by PRM in bioUb pull-down elutions of control and UBE3A overexpressing mice brains is indicated. The area quantified corresponding to the endogenous peptides as well as SIL peptides is shown. UBE3A/Control ratio of endogenous and SIL peptides is calculated, as well as the normalized endogenous/SIL ratio

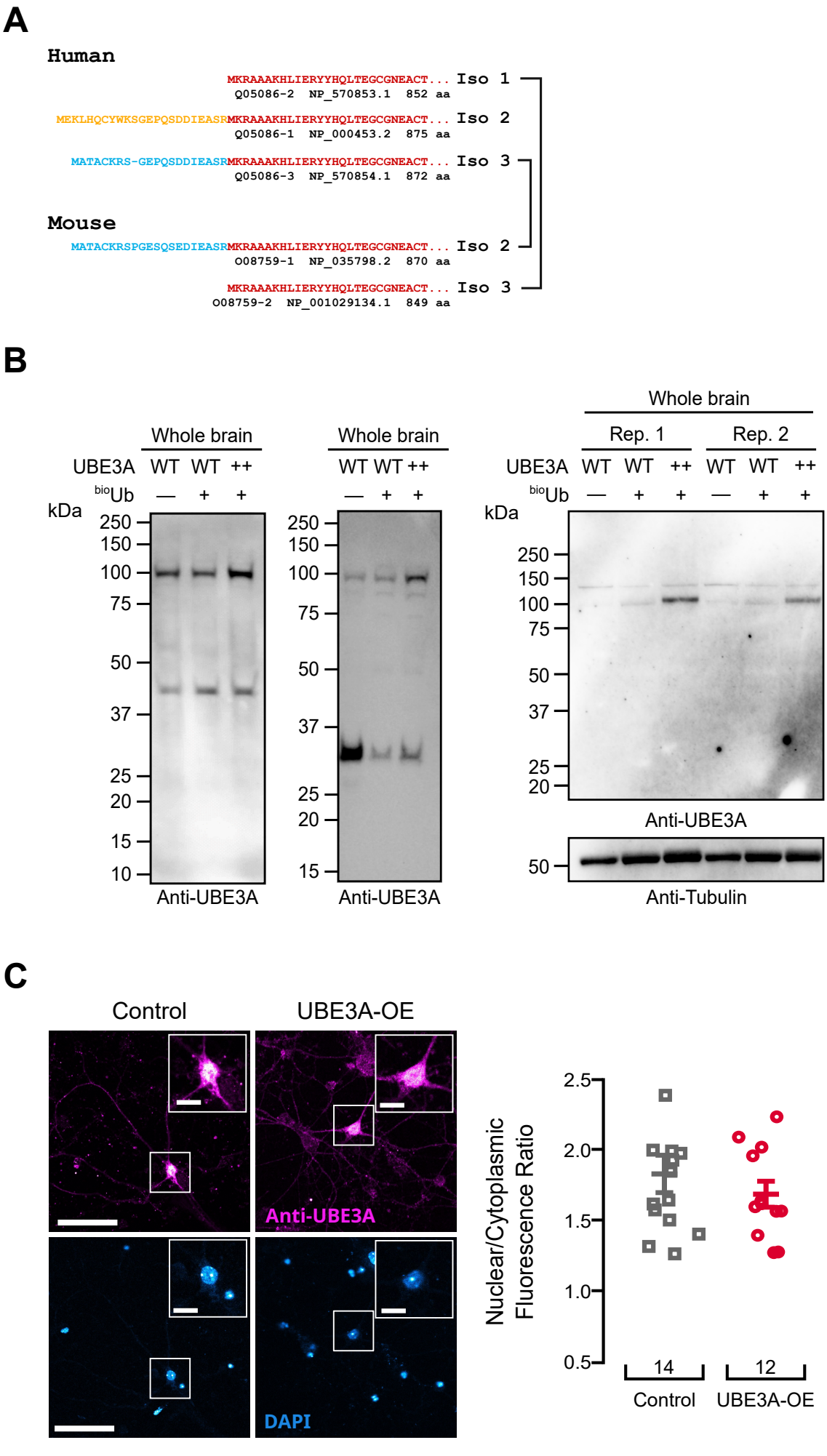

Supplementary Figure 1

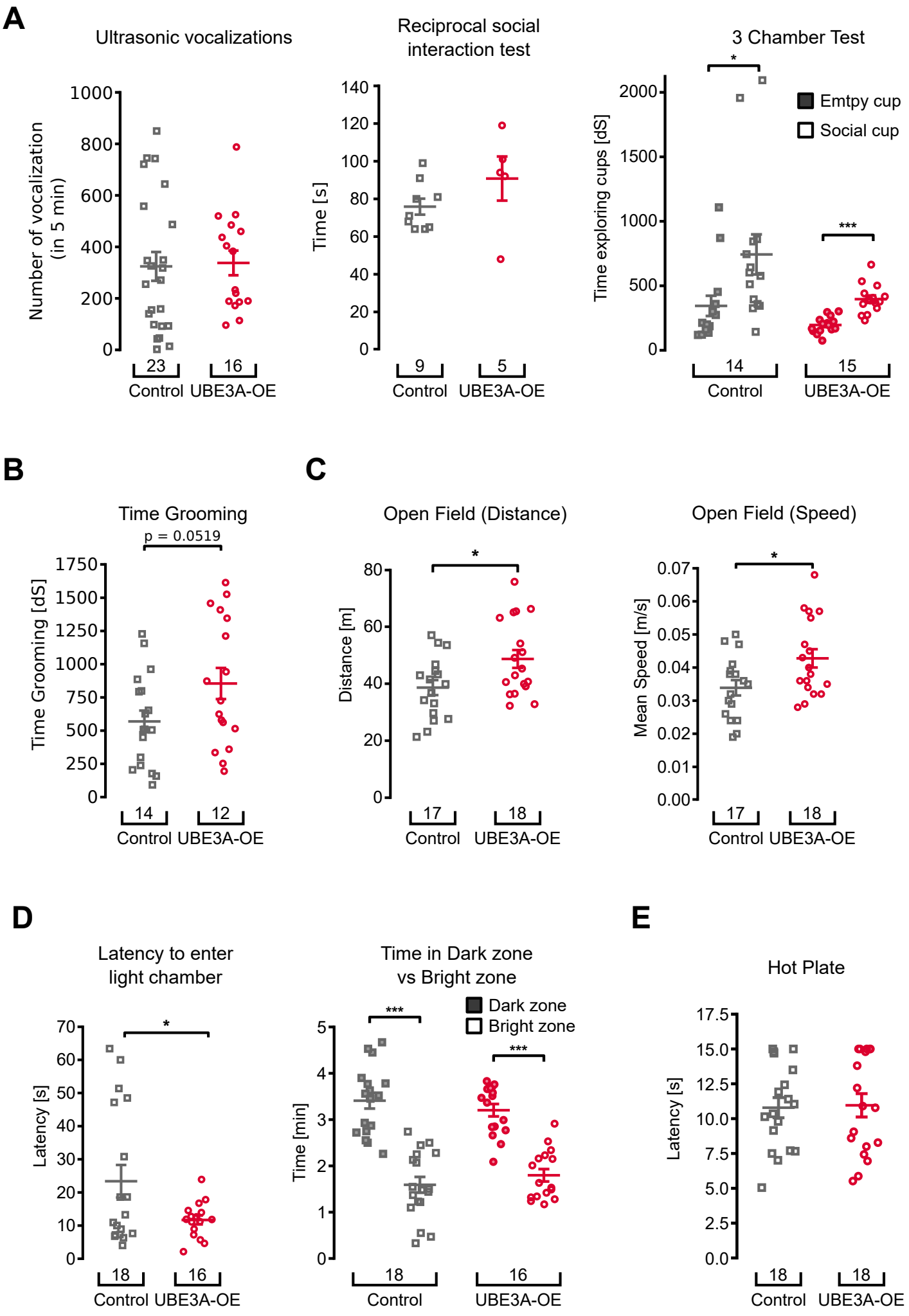

Supplementary Figure 2

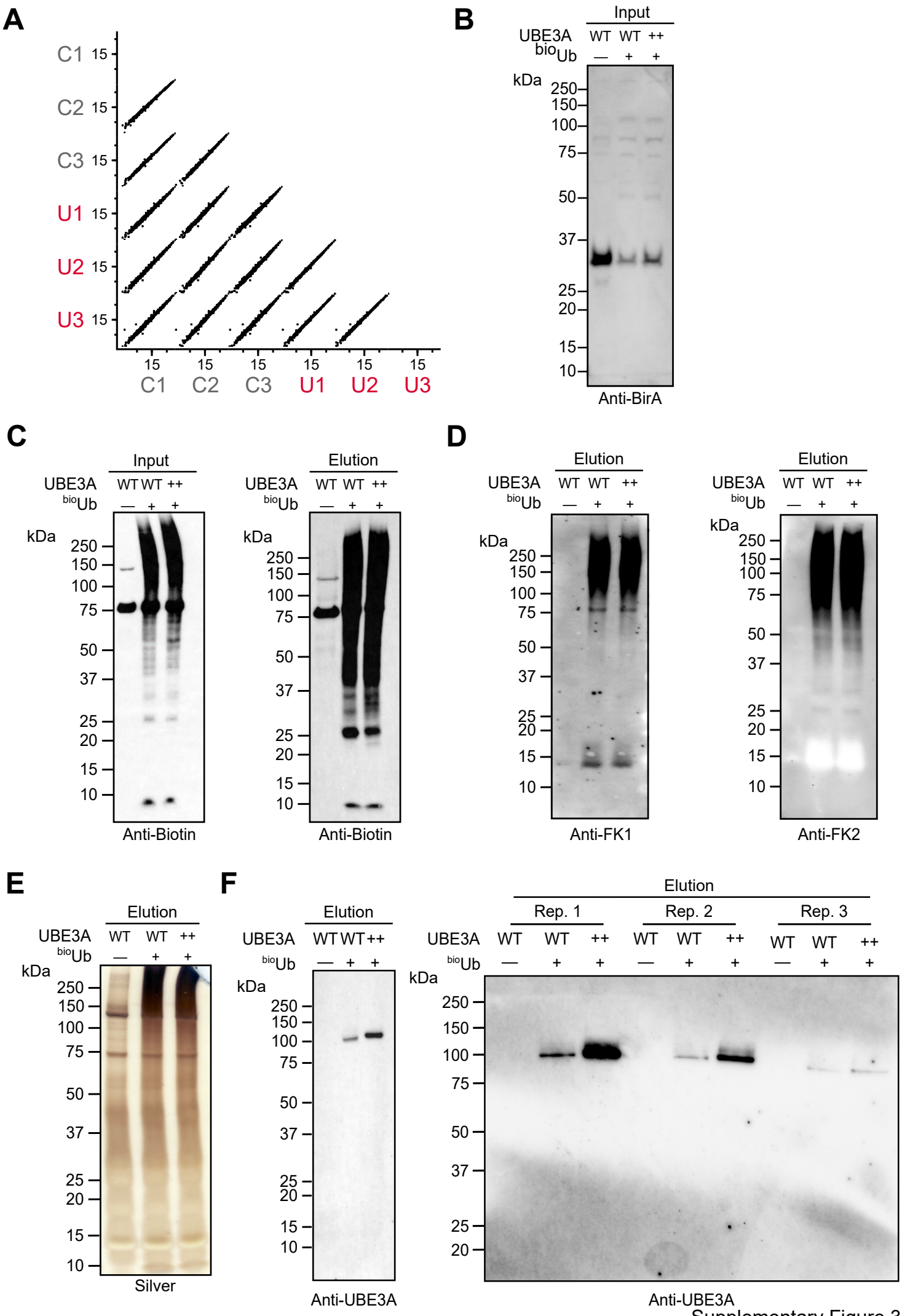

Supplementary Figure 3

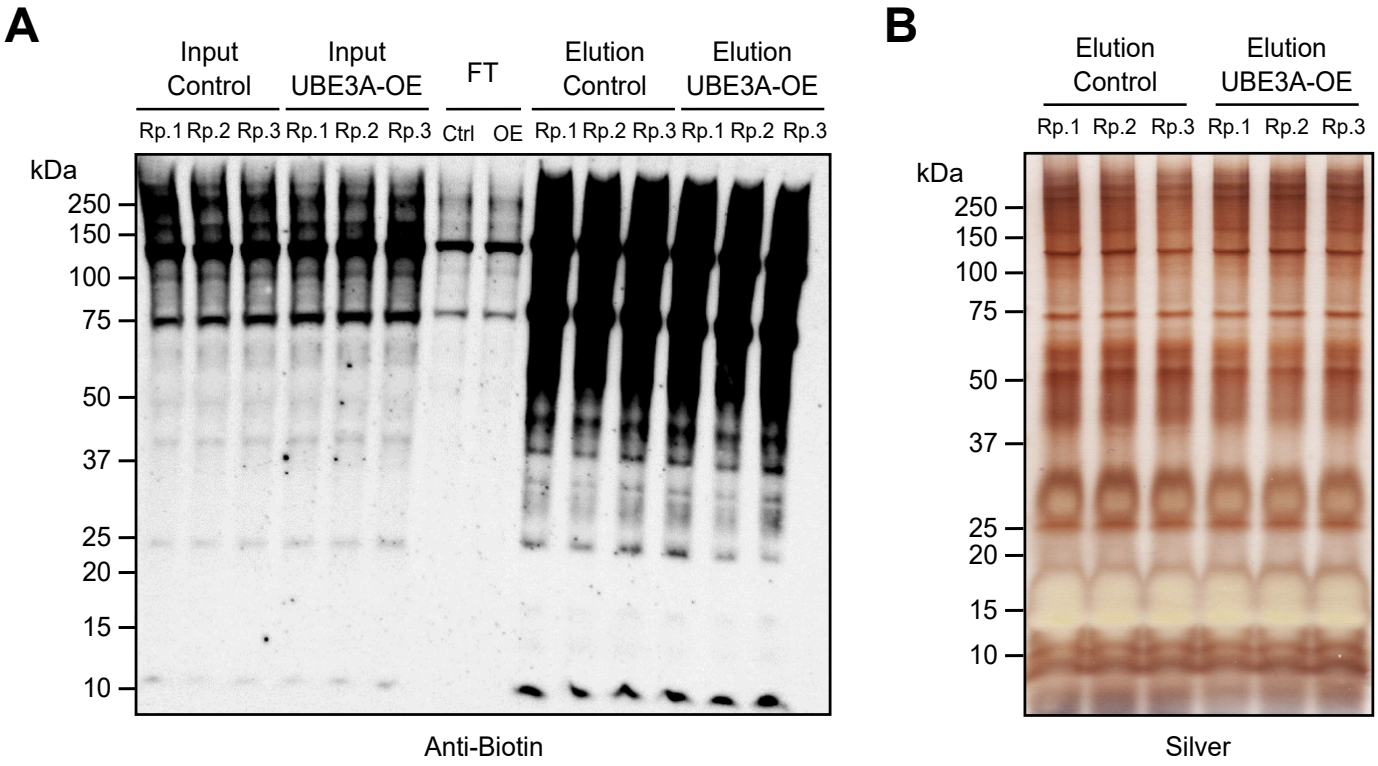

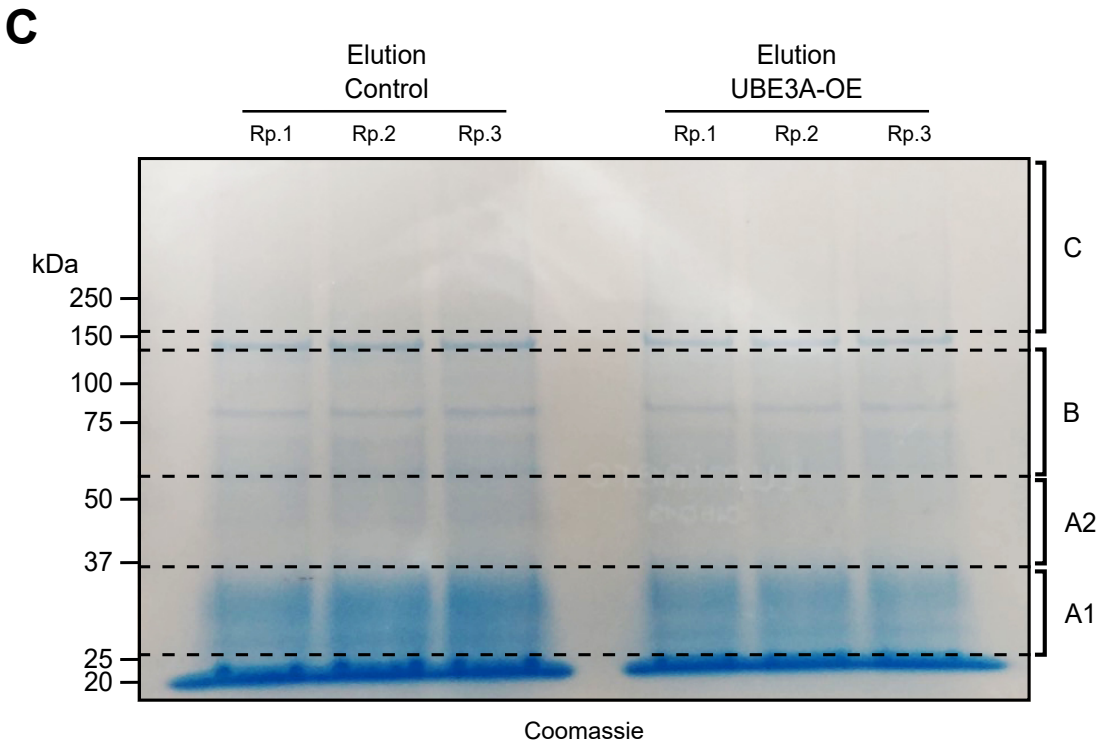

Supplementary Figure 4

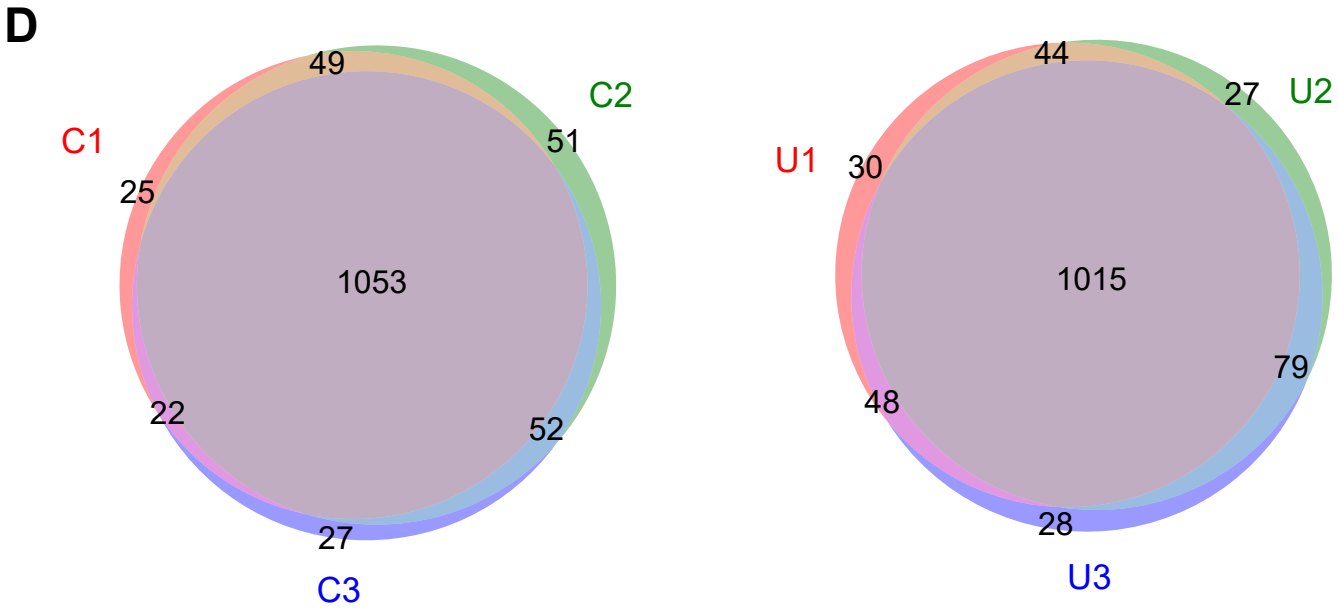
D
C1
C2
C3
49
51
25
1053
22
52
27
U1
U2
U3
44
27
30
1015
79
48
28

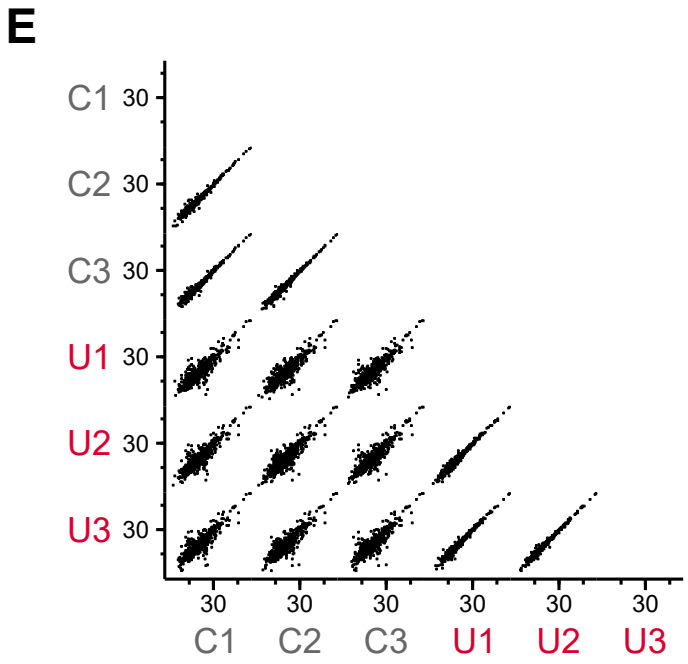
E
C1 30
C2 30
C3 30
U1 30
U2 30
U3 30
30 30 30 30 30 30
C1 C2 C3 U1 U2 U3

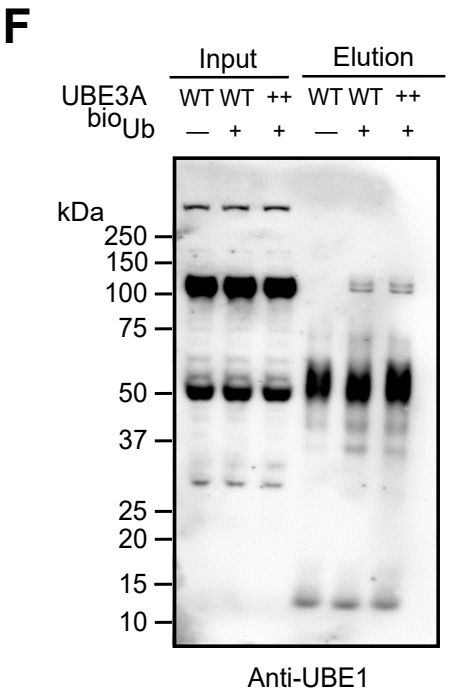
F
Input
Elution
UBE3A WT WT ++ WT WT ++
bioUb — + + — + +
kDa
250
150
100
75
50
37
25
20
15
10
Anti-UBE1

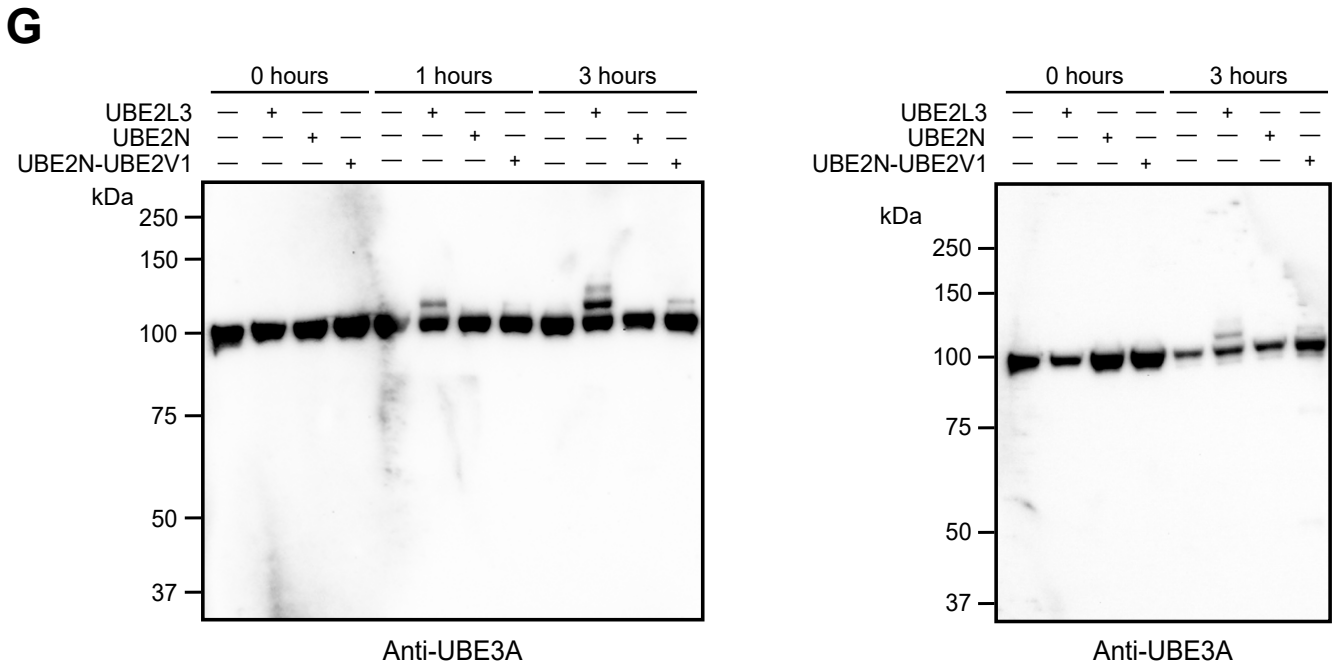
G
0 hours
1 hours
3 hours
UBE2L3
UBE2N
UBE2N-UBE2V1
kDa
250
150
100
75
50
37
Anti-UBE3A
0 hours
3 hours
UBE2L3
UBE2N
UBE2N-UBE2V1
kDa
250
150
100
75
50
37
Anti-UBE3A

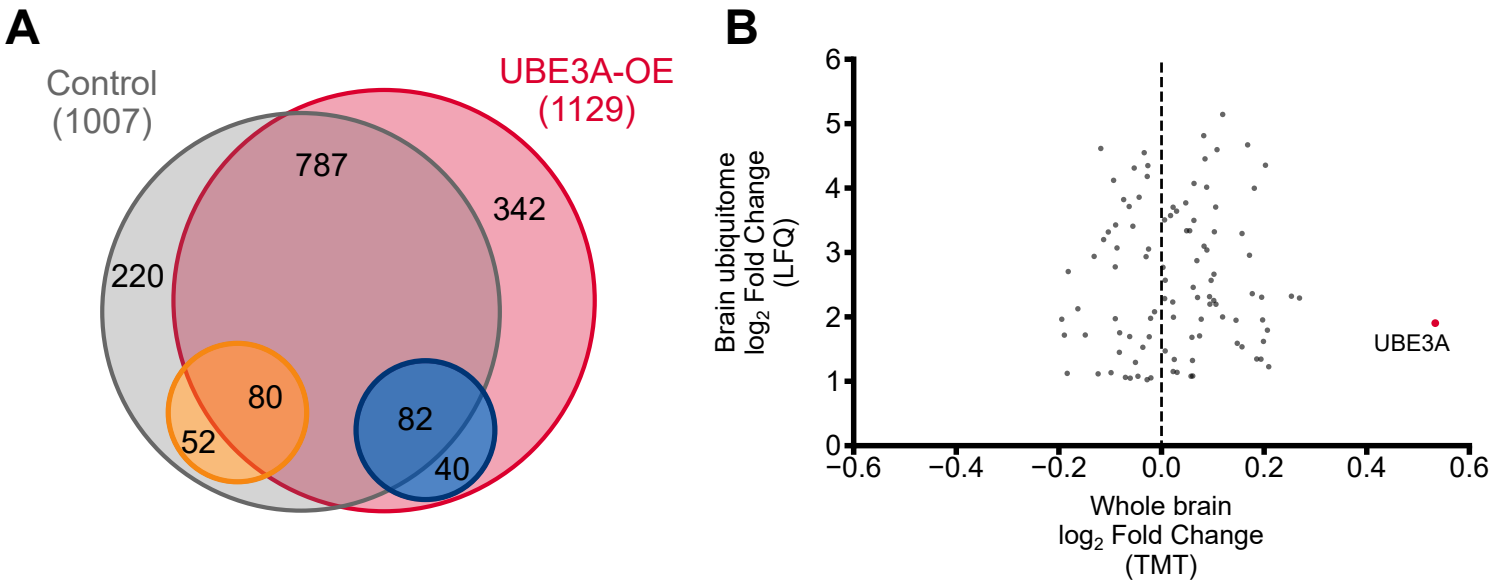

Supplementary Figure 5

A

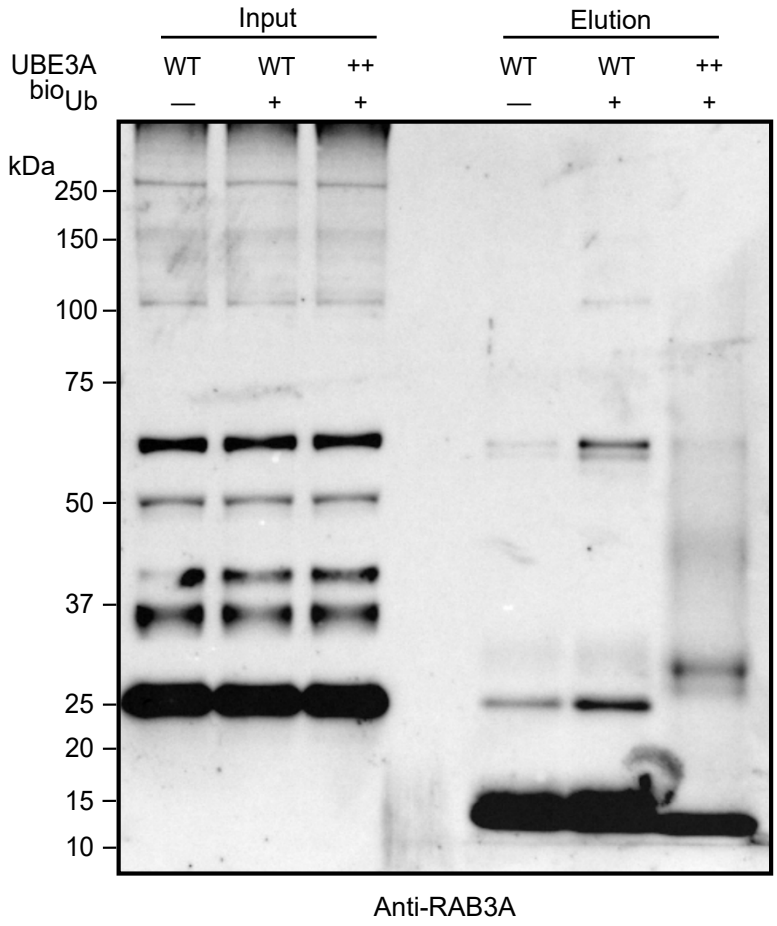

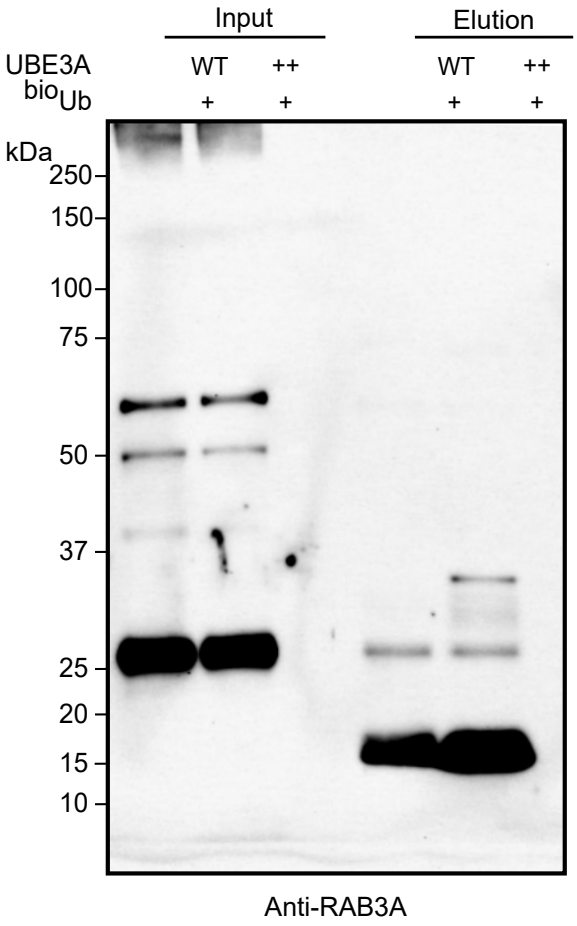

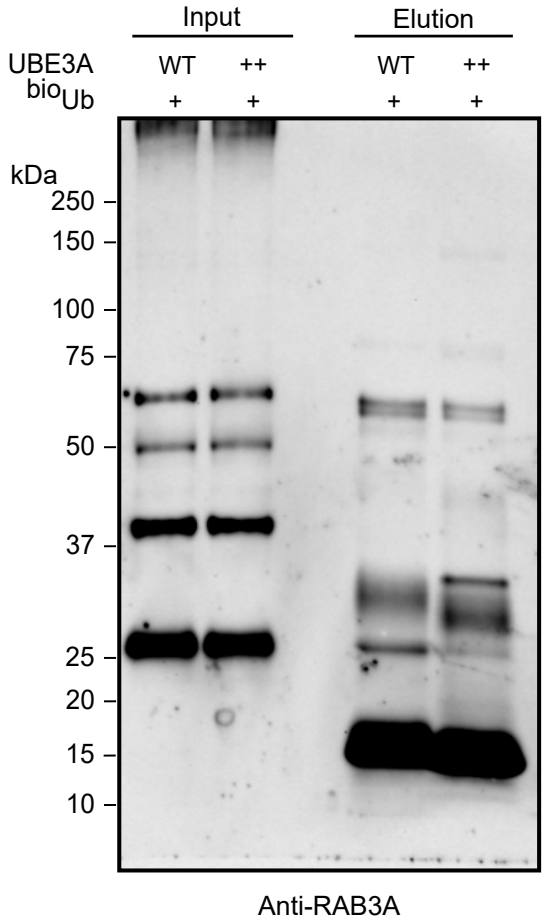

Supplementary Figure 6

B

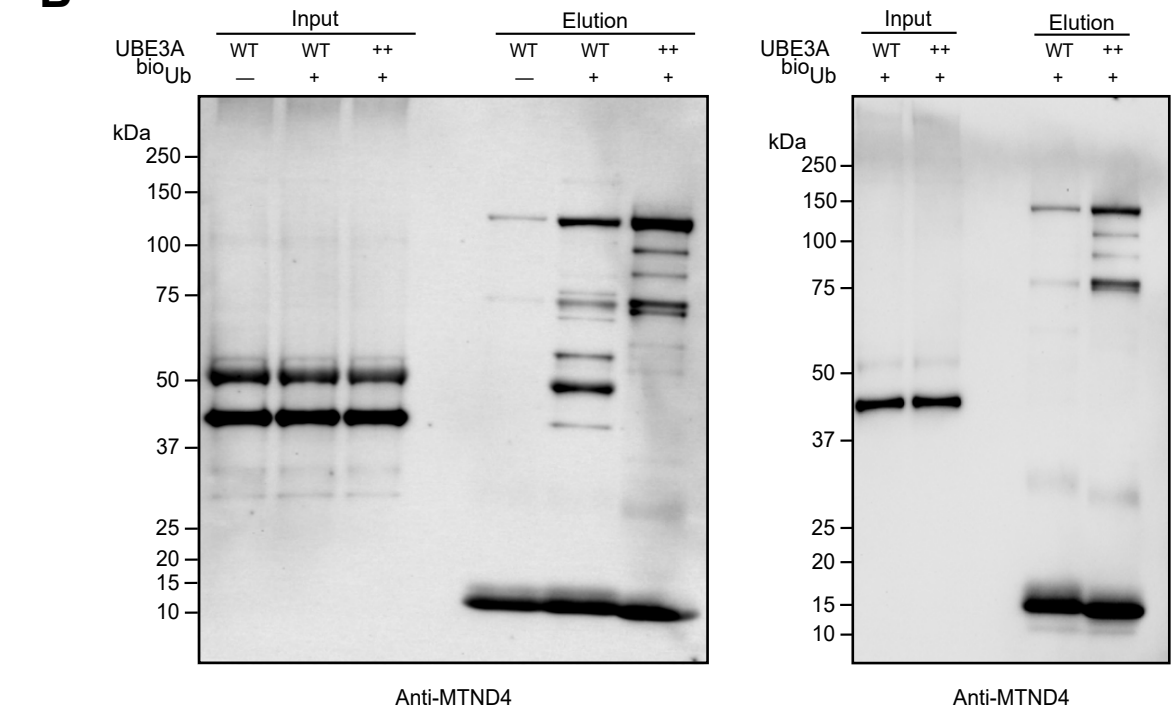
Input
Elution
UBE3A
bioUb
WT
WT
++
—
+
+
kDa
250
150
100
75
50
37
25
20
15
10
Anti-MTND4

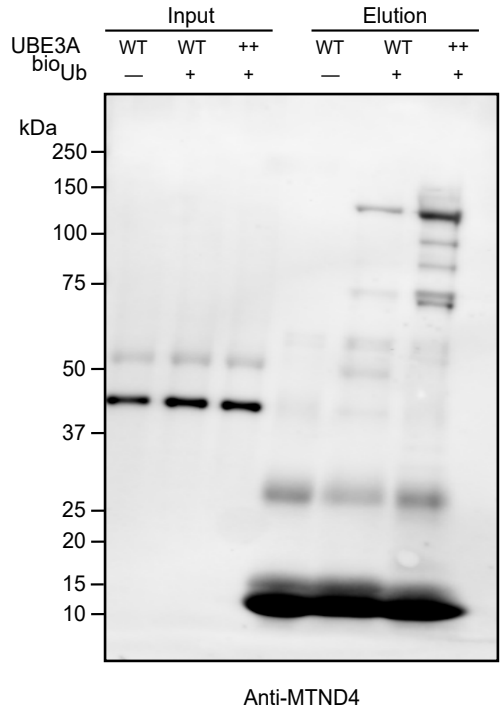
Input
Elution
UBE3A
bioUb
WT
WT
++
—
+
+
kDa
250
150
100
75
50
37
25
20
15
10
Anti-MTND4

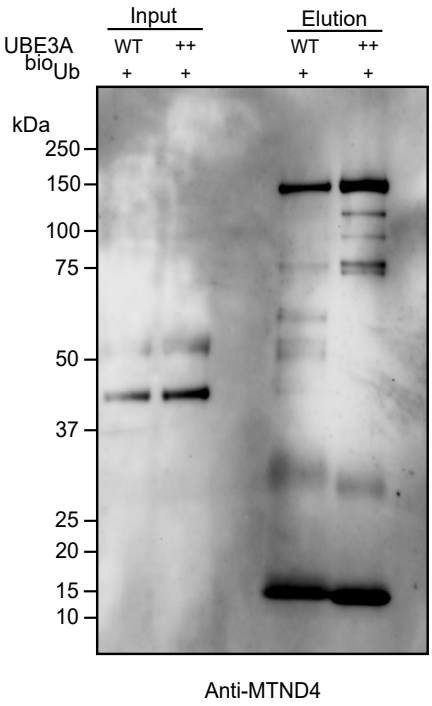
Input
Elution
UBE3A
bioUb
WT
++
+
+
kDa
250
150
100
75
50
37
25
20
15
10
Anti-MTND4

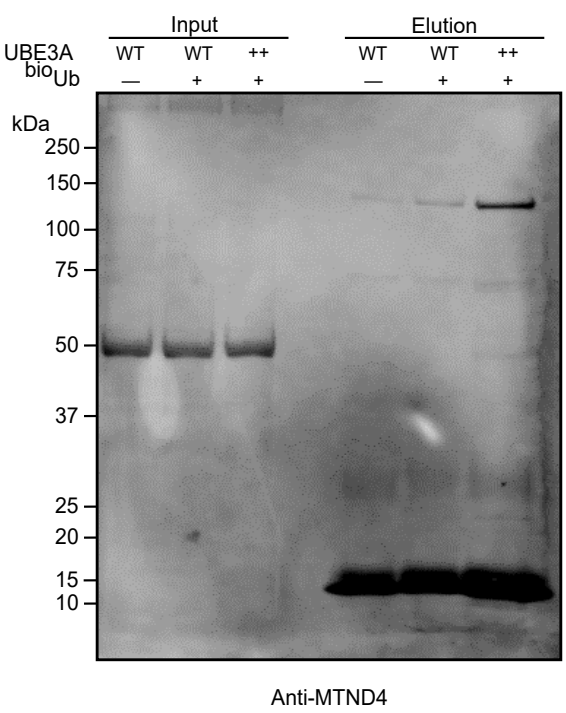
Input
Elution
UBE3A
bioUb
WT
WT
++
—
+
+
kDa
250
150
100
75
50
37
25
20
15
10
Anti-MTND4

C

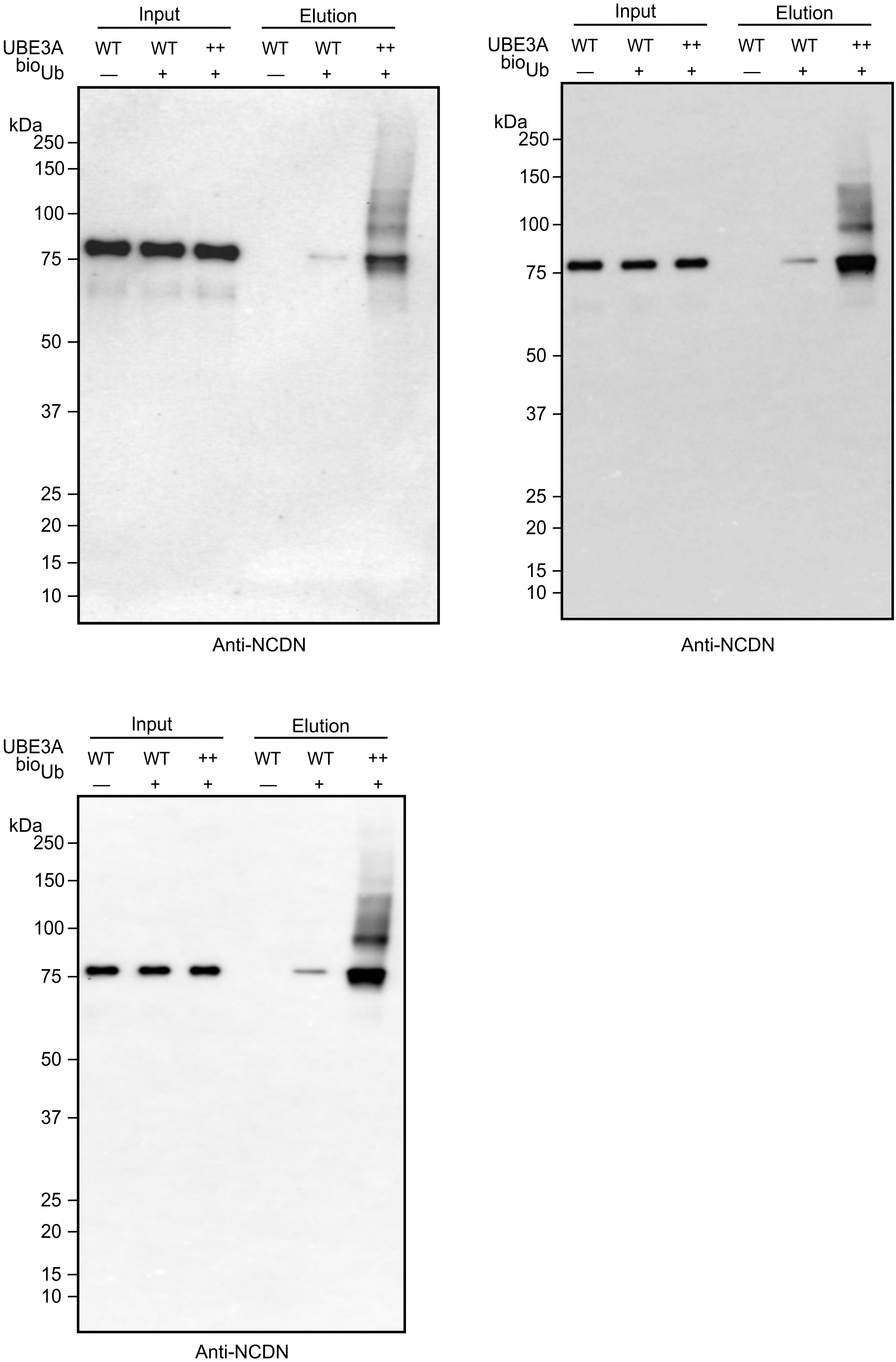
Input
Elution
UBE3A WT WT ++ WT WT ++
bioUb — + + — + +
kDa
250
150
100
75
50
37
25
20
15
10
Anti-NCDN
Input
Elution
UBE3A WT WT ++ WT WT ++
bioUb — + + — + +
kDa
250
150
100
75
50
37
25
20
15
10
Anti-NCDN
Input
Elution
UBE3A WT WT ++ WT WT ++
bioUb — + + — + +
kDa
250
150
100
75
50
37
25
20
15
10
Anti-NCDN

D

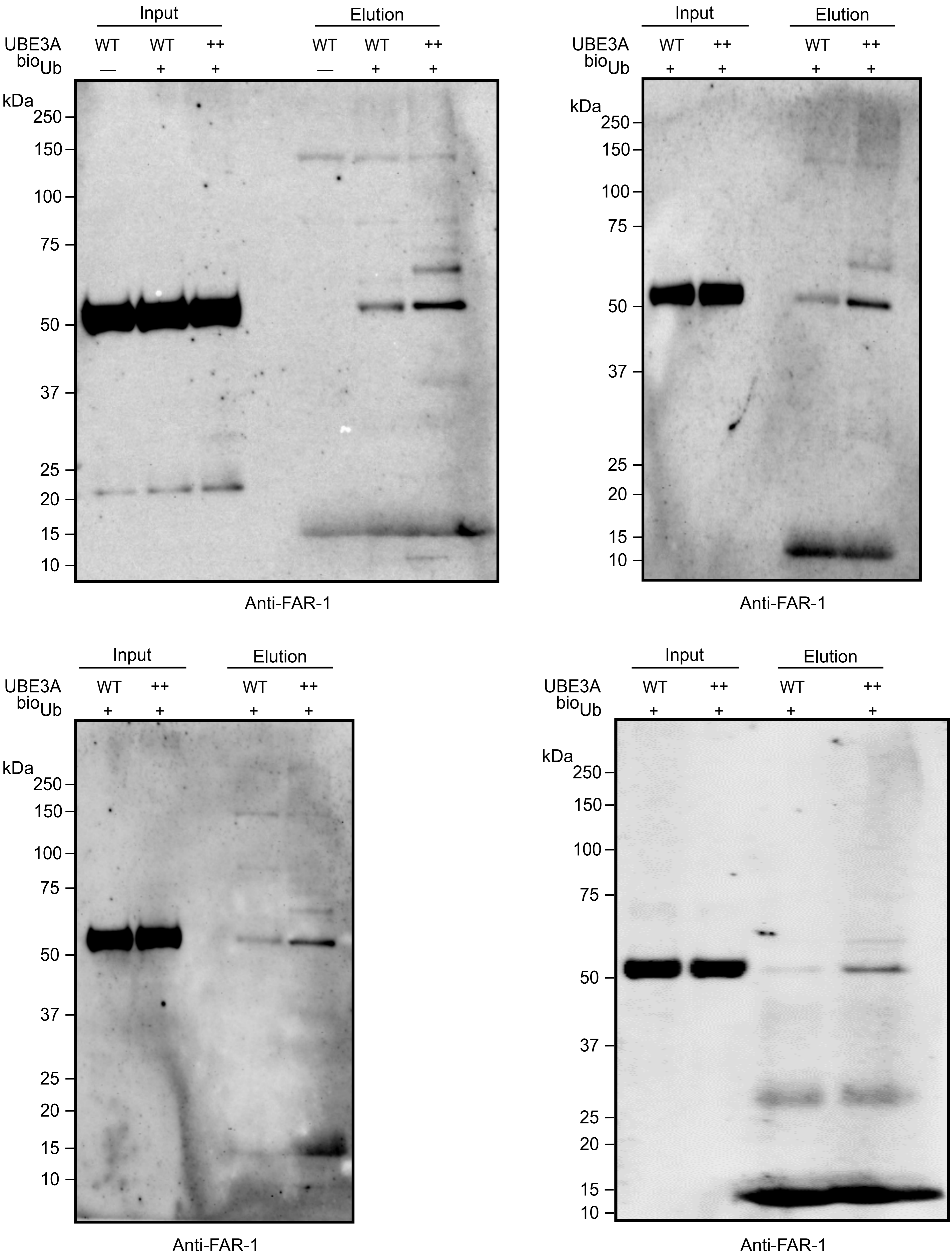
Input
Elution
UBE3A WT WT ++ WT WT ++
bioUb — + + — + +
kDa
250
150
100
75
50
37
25
20
15
10
Anti-FAR-1
Input
Elution
UBE3A WT ++ WT ++
bioUb + + + +
kDa
250
150
100
75
50
37
25
20
15
10
Anti-FAR-1
Input
Elution
UBE3A WT ++ WT ++
bioUb + + + +
kDa
250
150
100
75
50
37
25
20
15
10
Anti-FAR-1
Input
Elution
UBE3A WT ++ WT ++
bioUb + + + +
kDa
250
150
100
75
50
37
25
20
15
10
Anti-FAR-1

E

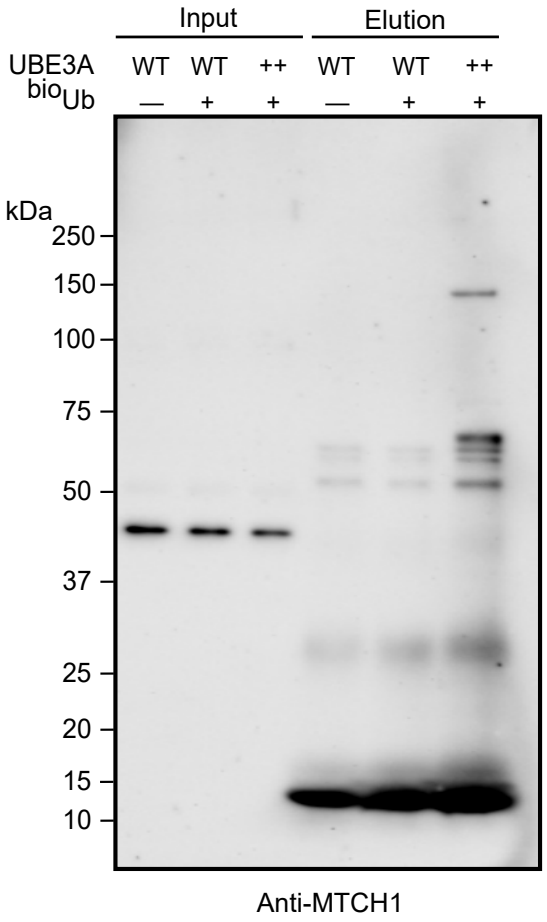
Input
Elution
UBE3A
WT WT ++ WT WT ++
bioUb
— + + — + +
kDa
250
150
100
75
50
37
25
20
15
10
Anti-MTCH1

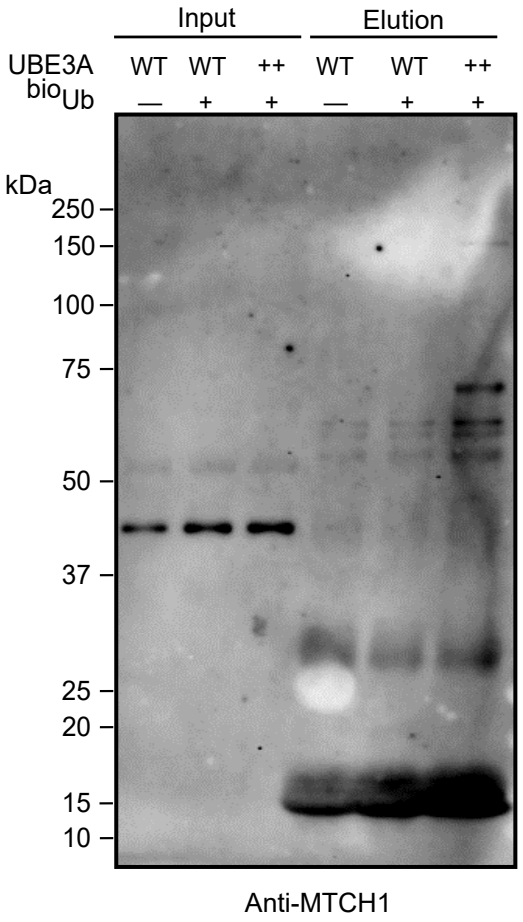
Input
Elution
UBE3A
WT WT ++ WT WT ++
bioUb
— + + — + +
kDa
250
150
100
75
50
37
25
20
15
10
Anti-MTCH1

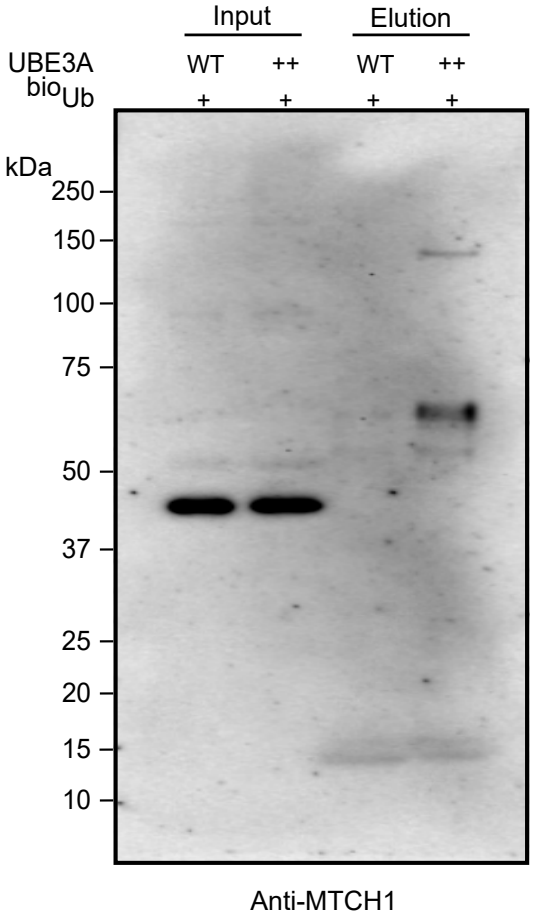
Input
Elution
UBE3A
WT ++ WT ++
bioUb
+ + + +
kDa
250
150
100
75
50
37
25
20
15
10
Anti-MTCH1

F

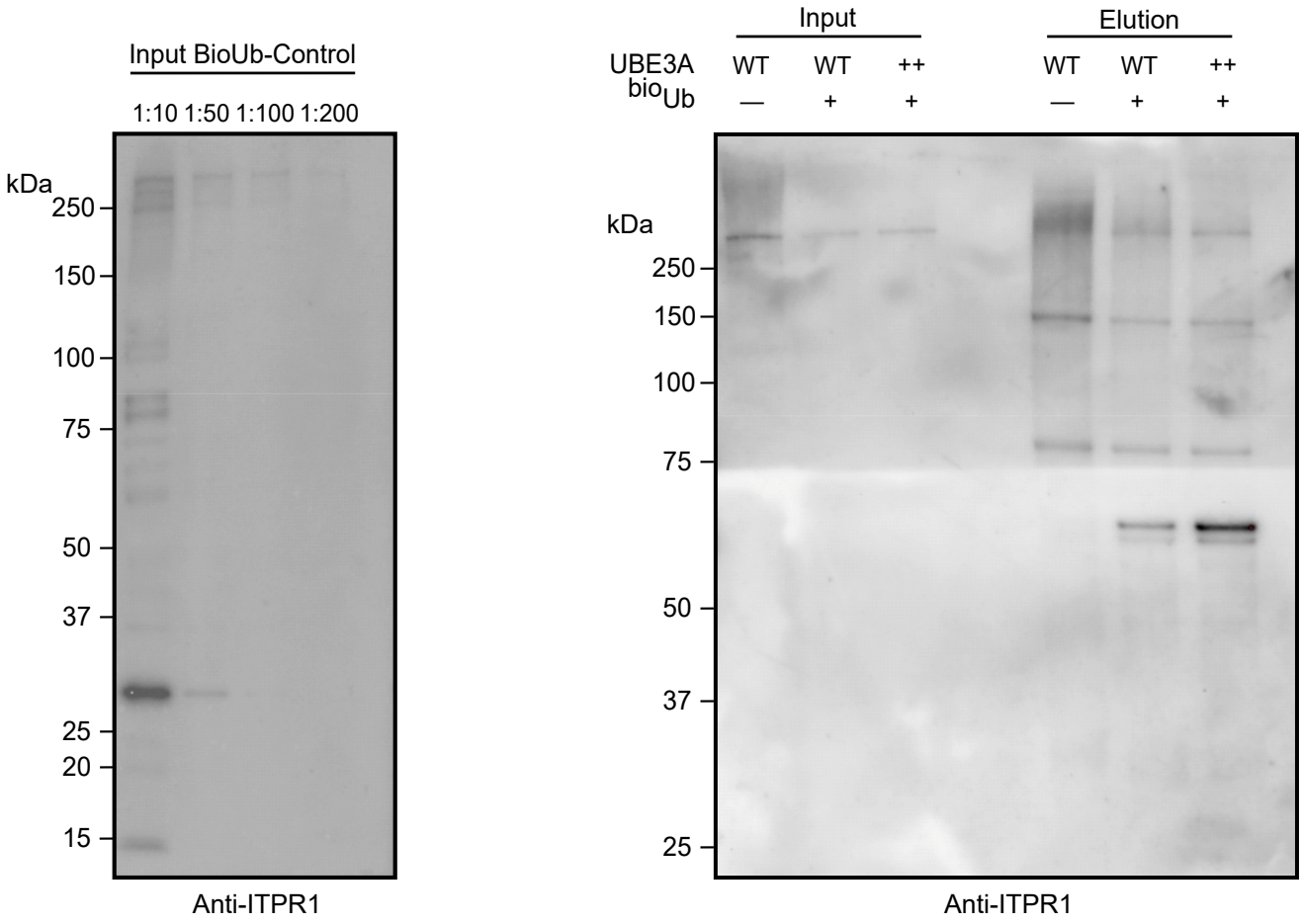
Input BioUb-Control
1:10 1:50 1:100 1:200
kDa
250
150
100
75
50
37
25
20
15
Anti-ITPR1
Input
Elution
UBE3A
WT
WT
++
WT
WT
++
bioUb
—
+
+
—
+
+
kDa
250
150
100
75
50
37
25
Anti-ITPR1